



OPEN

SUBJECT AREAS:

MIRNAS

EPILEPSY

Received
16 December 2013Accepted
1 April 2014Published
22 April 2014

Correspondence and requests for materials should be addressed to J.-T.Y. (yu-jintai@163.com) or L.T. (dr.tanlan@163.com)

* These authors contributed equally to this work.

Genome-wide microRNA expression profiles in hippocampus of rats with chronic temporal lobe epilepsy

Meng-Meng Li^{1*}, Teng Jiang^{2*}, Zhen Sun³, Qun Zhang¹, Chen-Chen Tan¹, Jin-Tai Yu^{1,2,3} & Lan Tan^{1,2,3}

¹Department of Neurology, Qingdao Municipal Hospital, School of Medicine, Qingdao University, Qingdao, China, ²Department of Neurology, Qingdao Municipal Hospital, Nanjing Medical University, Qingdao, China, ³Department of Neurology, Qingdao Municipal Hospital, Taishan Medical University, Qingdao, China.

The expression and functions of microRNAs (miRNAs) in chronic temporal lobe epilepsy (TLE), the most common type of refractory epilepsy in adults, are poorly understood currently. In this study, status epilepticus evoked by amygdala stimulation was used to establish rat chronic TLE model. Two months later, high-throughput sequencing was employed to investigate miRNA expression profile in rat hippocampus, and six miRNAs were confirmed to be differentially expressed. Kyoto Encyclopedia of Genes and Genomes pathway analysis indicated that most of the target genes for these six miRNAs were associated with neuronal apoptosis. Meanwhile, the levels of miR-423-3p and miR-296-5p were correlated with the activity of caspase-3, an apoptosis indicator. Additionally, the loading of miR-423-3p was increased in RNA-induced silencing complex whilst caspase-6, a target of miR-423-3p, was reduced in chronic TLE rats. Collectively, our findings suggest that miRNAs may exert anti-apoptotic effects in chronic TLE.

Chronic temporal lobe epilepsy (TLE) is the most common type of partial epilepsy in adults¹. Symptoms in chronic TLE consist of partial or generalized seizures that originate from the amygdala many years after an initial brain insult such as status epilepticus (SE), encephalitis or febrile convulsions^{2,3}. To date, the underlying molecular mechanisms of chronic TLE are still unclear. MicroRNAs (miRNA) are small non-coding RNAs that regulate the expression of target genes by binding to the 3'-untranslated regions of target mRNA⁴. In mammals, more than 50% of all miRNAs are expressed in the brain⁵, suggesting a particularly significant role for miRNAs in brain physiology^{6,7}. In recent years, accumulating evidence suggested that miRNA was implicated in the pathogenesis of epilepsy^{8,9}. Several studies indicated a differential expression of several miRNAs in brain of SE patients and animal models¹⁰⁻¹². Meanwhile, by employing rat model of SE, our group and Hu et al. have demonstrated that several differentially expressed miRNAs were involved in modulation of neuronal apoptosis, a main pathological characteristics of SE^{13,14}.

Considering the above evidence, we hypothesized that refractory epilepsy such as chronic TLE also led to dramatic alterations in brain miRNA levels, and dysregulation of miRNA might be associated with neuronal apoptosis and brain damages in chronic TLE. In order to test this hypothesis, we employed high-throughput sequencing to investigate the miRNA expression profiles in hippocampus of chronic TLE rats. Meanwhile, Nissl staining was used to detect neuronal losses whilst terminal deoxynucleotidyl transferase-mediated dUTP end-labeling (TUNEL) and the activity of caspase-3, an apoptosis indicator, were used to assess neuronal apoptosis in hippocampus. In addition, the association between differentially expressed miRNAs and caspase-3 activity was evaluated, and the loading of miRNAs in RNA-induced silencing complex (RISC) as well as the protein levels of their predict targets were also determined here. It should be noted that we induced chronic TLE in rats by using amygdala stimulation in this study, as this model could mimic behavioral, electroencephalographic, and morphological phenomena of human chronic TLE better than chemoconvulsants-induced TLE model¹⁵⁻¹⁷.

Results

We obtained 8,839,947 and 9,080,314 raw reads from control group and chronic TLE group, respectively. As demonstrated by Supplementary Fig. S1, the most abundant size class was 22 nt, which accounted for 60.97% (control group) and 48% (chronic TLE group) of the total reads, respectively. After discarding the sequences shorter than 18 nt and low-quality sequences, 8,736,906 and 8,930,938 clean reads of 18–30 nt from the control group and chronic TLE group, respectively, were obtained for subsequent analysis.

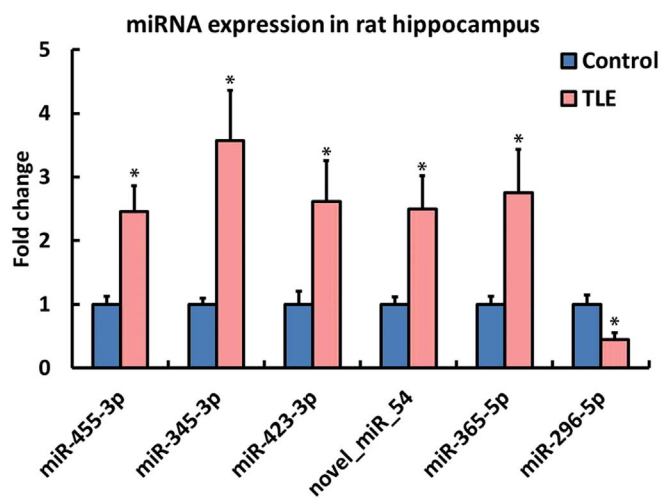


Figure 1 | Confirmation of six differentially expressed miRNAs using qRT-PCR at 2 months after amygdala stimulation. The expression of all genes is normalized to the levels of U6 snoRNA; Data are presented as the mean \pm SD; * $P < 0.05$ versus control group; $n = 6$ per group.

The expression patterns of known miRNA in rat hippocampus at 2 months after amygdala stimulation were indicated by Supplementary Fig. S2. We identified novel miRNAs at 2 months after amygdala stimulation by using miRDeep software, which was designed to uncover novel miRNAs in deep sequencing data as previously described^{18,19}. The algorithm of miRDeep took into account several factors to score the probability that a candidate small RNA represented a *bona fide* miRNA: (1) the presence in the deep sequencing data of reads corresponding to typical products of miRNA biogenesis; (2) the stability of the putative premiRNA hairpin; and (3) homology to previously identified miRNAs. After discarding reads corresponding to previously annotated regions, miRDeep analysis revealed the existence of a total of 63 novel miRNAs (Fig. S3).

After comparing the miRNA expression profile in control group and chronic TLE group, we detected 25 miRNAs that were differentially expressed in rat hippocampus. Among these miRNAs, fourteen miRNAs were found to be up-regulated whilst eleven miRNAs were down-regulated (Supplementary Table S1). Afterwards, six miRNAs (miR-455-3p, miR-345-3p, miR-423-3p, novel miR-54, miR-365-5p, and miR-296-5p) were screened out based on the criteria mentioned in “Methods” section, and qRT-PCR was performed to validate the alterations of these miRNA. As shown in Fig. 1, at 2 months after amygdala stimulation, the expression of miR-455-3p, miR-345-3p, miR-423-3p, novel miR-54, and miR-365-5p was significantly increased ($P < 0.05$) while the levels of miR-296-5p was markedly decreased in rat hippocampus ($P < 0.05$). These findings were consistent with results from high-throughput sequencing.

To predict the function of the six differentially expressed miRNAs that confirmed by qRT-PCR, the RNAhybrid and miRanda algorithms were used to obtain a list of potential target genes. Subsequent Kyoto Encyclopedia of Genes and Genomes (KEGG) pathway analysis indicated that most of the predicted target genes such as Fadd, Fas, Casp, and Bax were closely relevant to neuronal apoptosis (Figure 2). Hence, these six miRNAs may play an important role in pathogenesis of chronic TLE by modulation of neuronal apoptosis in hippocampus.

We then employed Nissl staining to investigate the neuronal survival rate in rat hippocampus. As shown by Fig. 3A, in rats with chronic TLE, a dramatic reduction of the neuronal survival rate was observed in CA1 and CA3 regions of hippocampus at 2 months after amygdala stimulation. To further investigate whether apoptosis was involved in chronic TLE-induced neuronal losses, we performed TUNEL assay to evaluate neuronal apoptosis rate in rat

hippocampus. As indicated by Fig. 3B, in hippocampus of chronic TLE rats, a significant increase in neuronal apoptosis rate was noted in CA1 and CA3 regions at 2 months after amygdala stimulation. In addition, we found that the activity of caspase-3, an indicator of apoptosis, was significantly higher in hippocampus of chronic TLE rats than that of controls (Fig. 3C). These results suggested that apoptosis represented part of the mechanisms underlying the chronic TLE-induced neuronal losses in hippocampus.

To evaluate whether the selected miRNAs were implicated in chronic TLE-induced neuronal apoptosis, we assessed the correlation between these six miRNAs and the caspase-3 activity in rat hippocampus at 2 months after amygdala stimulation. Pearson’s correlation analysis showed a positive correlation between miR-423-3p and caspase-3 activity in hippocampus (Fig. 3D, $r = 0.874$, $P = 0.023$). In addition, a negative correlation was found between miR-296-5p and activity of caspase-3 (Fig. 3D, $r = -0.881$, $P = 0.02$). These data indicated that miR-423-3p and miR-296-5p might be implicated in the regulation of neuronal apoptosis in chronic TLE.

Subsequently, we investigated whether miR-423-3p exerted its function in brain of chronic TLE rats. We selected miR-423-3p rather than miR-296-5p mainly because its alteration is more apparent than that of miR-296-5p in chronic TLE (shown in Fig. 1). To determine whether up-regulation of miR-423-3p led to a corresponding increment in loading of the miRNA into the RISC, we immunoprecipitated Argonaute (Ago)-2, a crucial component of RISC, from hippocampus of controls and chronic TLE rats. It should be noted that no significant difference was observed in Ago-2 levels between controls and chronic TLE rats (Fig. 4A). As demonstrated by Fig. 4B, the levels of miR-423-3p bound to Ago-2 were dramatically increased in hippocampus of chronic TLE rats when compared with those of controls. Meanwhile, western blot analysis indicated a significant reduction in protein levels of caspase-6, a predicted target of miR-423-3p (shown in Fig. 2), in hippocampus of chronic TLE rats in comparison to controls (Fig. 4C).

Discussion

Here, we provided the first evidence that chronic TLE induced by amygdala stimulation led to dramatic changes in the miRNA expression profile in rat hippocampus. Five miRNAs including miR-455-3p, miR-345-3p, miR-423-3p, novel miR-54, and miR-365-5p were significantly increased whilst miR-296-5p was remarkably decreased in brain at 2 months after amygdala stimulation. These observations were in agreement with a previous study from Risbud and colleagues, as they found that miR-423-3p was up-regulated in a chronic TLE model induced by pilocarpine²⁰. In addition, our findings were also supported by a recent study from Hu et al., as miR-296-5p was revealed to be down-regulated in rats with chronic TLE¹³. Interestingly, in contrast to our results, the expression of miR-455-3p, miR-345-3p, miR-423-3p, novel miR-54, and miR-365-5p remained unchanged in a recent study from Gorter and colleagues¹⁵. Meanwhile, Bot et al. found a moderate but significant reduction in miR-345-3p in rats with chronic TLE¹⁶. The lack of reproducibility in the miRNA expression profile can be explained by the diversity in TLE models, time-point, and the criteria for miRNA screening. Of note, the miRNA expression was profiled using microarrays in studies from Gorter et al. and Bot et al., whereas we employed high-throughput sequencing to characterized miRNA expression here^{15,16}. The differences in the sensibility and specificity between microarrays and high-throughput sequencing may also be responsible for these contradictory findings. It should be noted that another study from our group indicated that miR-345-3p and miR-365-5p were also dramatically increased in rats with status epilepticus, implying that miRNAs play a crucial role not only in chronic TLE but also in other types of epilepsy¹⁴. Nevertheless, the expression of miR-345-3p and miR-365-5p was increased at 24 hour and started to be recovered at 3 weeks after onset of SE whilst that was up-regulated at 2 month after

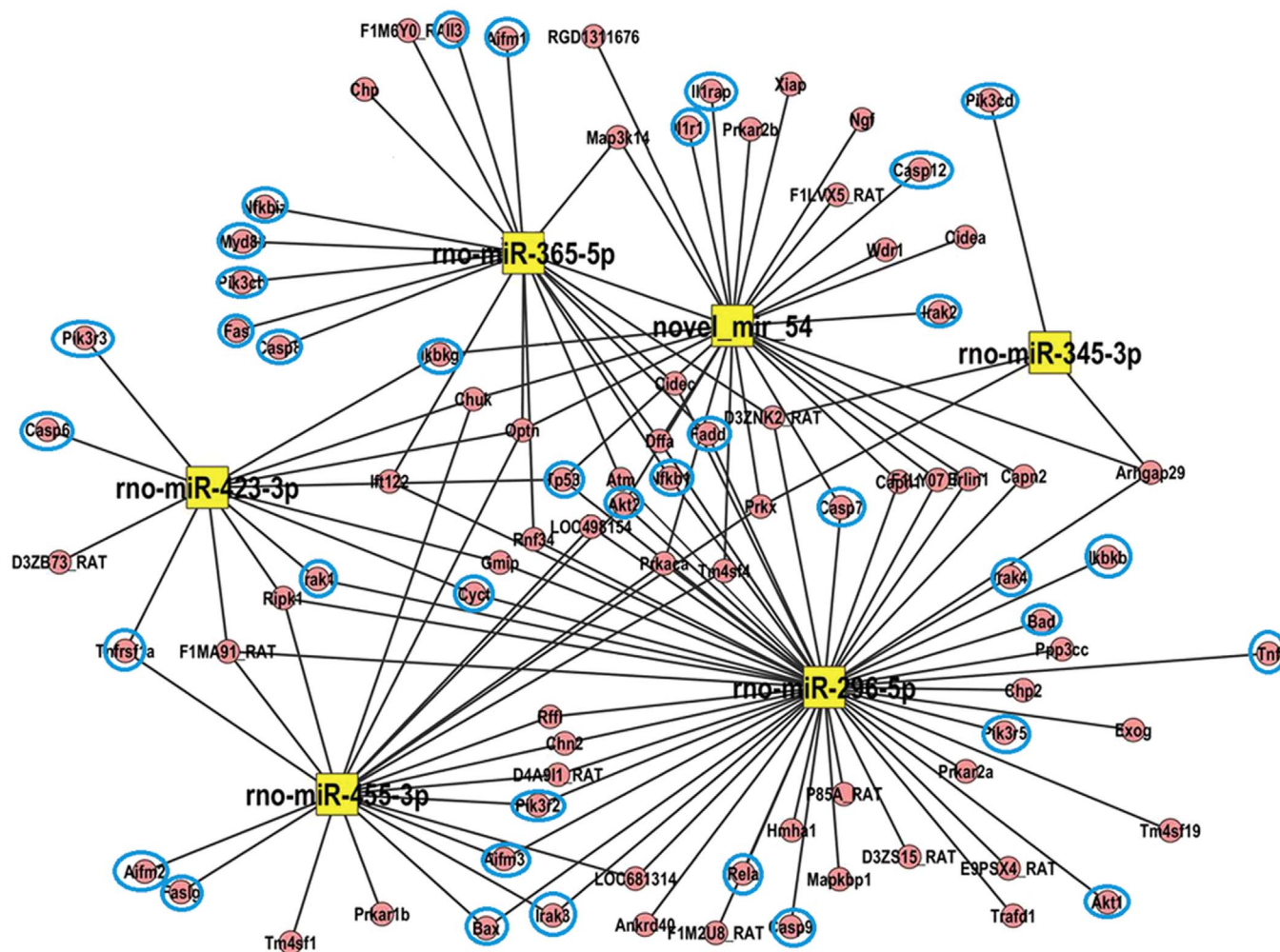


Figure 2 | Genes potentially targeted by six differentially expressed miRNAs. Boxes in yellow represent miRNAs, whereas cycles in red represent mRNAs. Apoptosis-related mRNAs are indicated by blue cycles.

induction of chronic TLE, possibly attributing to the differences in pathophysiology mechanisms underlying these two types of epilepsy.

As a form of programmed cell death, apoptosis was implicated in chronic TLE-induced neuron losses and brain damage^{12,21–24}. In the current study, we found that chronic TLE dramatically increased the number of apoptotic neurons in rat hippocampus. These findings were supported by a recent study from Hu et al., which demonstrated that apoptosis represents part of the mechanisms underlying the chronic TLE-induced neuronal losses¹³. Chronic TLE-induced apoptosis can be triggered by activation of intrinsic pathway components including pro-apoptotic proteins belonging to Bcl-2 and caspase family. In addition, the extrinsic pathway mediated by TNFR1 and Fas is also found to be activated following chronic TLE and triggers neuronal apoptosis^{25,26}. Interestingly, the subsequent KEGG pathway analysis indicated that these six miRNAs were targeted to genes involved in both intrinsic and extrinsic pathway of apoptosis, such as Fas, Casp6, Casp9, and Bax. Meanwhile, we found that the expression of miR-423-3p and miR-296-5p were significantly correlated with the activity of caspase-3, an indicator of apoptosis, further implying that these miRNAs participate in the pathogenesis of chronic TLE by modulating neuronal apoptosis in hippocampus. These findings were in agreement with a previous study from Hu and colleagues, which demonstrated expression of several miRNAs was dramatically changed and provided modulation on neuronal apoptosis in rats with chronic TLE¹³. More importantly, the loading of miR-423-3p was found to be increased in RISC where the miRNA-based RNA silencing occurred⁸. In addition, the protein levels of

caspase-6, a predicted target of miR-423-3p, showed expected reduction in hippocampus of chronic TLE rats. These results further implied that miR-423-3p might be compensatorily up-regulated in response to cellular apoptosis, and exerted anti-apoptotic effects in chronic TLE.

In conclusion, we employed high-throughput sequencing to characterize miRNA expression profile in hippocampus of rats with chronic TLE. Six miRNAs including miR-455-3p, miR-345-3p, miR-423-3p, novel miR-54, and miR-365-5p were confirmed to be differentially expressed at 2 months after amygdala stimulation. In addition, miR-423-3p and miR-296-5p were significantly correlated with neuronal apoptosis in hippocampus. Moreover, the loading of miR-423-3p was increased in RISC whilst the protein levels of caspase-6, a predicted target of miR-423-3p, showed expected reduction in hippocampus of chronic TLE rats. These findings indicate that miRNAs may provide protective effects against neuronal apoptosis in chronic TLE, and therapies targeting miRNA may open up new avenues for the treatment of refractory epilepsy.

Methods

Adult male Sprague–Dawley rats weighing 230–270 g were obtained from Experimental Animal Center of Qingdao University. They were allowed free access to food and water and were maintained on a 12 h light/dark cycle with a controlled temperature and humidity, and given free access to food and water. All experiments were performed in strict accordance with National Institute of Health Guide for the Care and Use of Laboratory Animals. Animal care and sacrifice were conducted according to methods approved by the Qingdao University Animal Experimentation Committee (permit No. QUEC-130629).

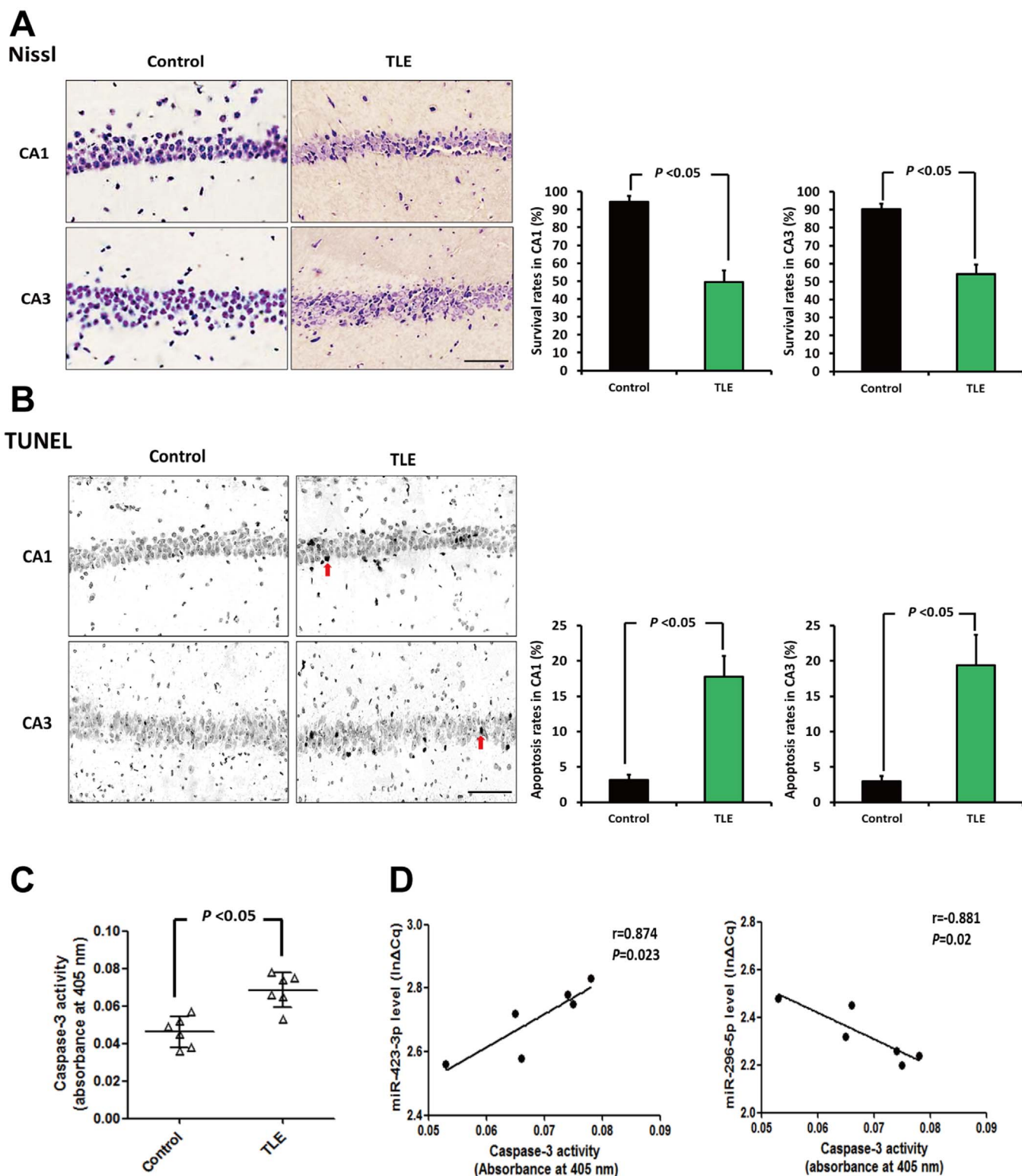


Figure 3 | Neuronal apoptosis in rat hippocampus and its correlation with miRNA levels at 2 months after amygdala stimulation. Neuronal survival was assessed by Nissl-staining. (A) Representative photo of Nissl-staining in CA1 region of rat hippocampus at 2 months after amygdala stimulation. Neurons with dark violet nucleus and intact morphology were identified as surviving neurons. Scale bars: 50 μ m. The neuronal survival rate was defined as follows: neuronal surviving rate (%) = $100 \times$ (count of surviving neurons/total count of neurons). Neuronal apoptosis was determined by TUNEL assay. (B) Representative photo of TUNEL in rat hippocampus at 2 months after amygdala stimulation. Photos were converted to black and white to obtain a better contrast ratio. Neurons with deep black nuclei were identified as TUNEL-positive cells (indicated by red arrows). Scale bars: 50 μ m. The neuronal apoptosis rate was defined as follows: neuronal apoptosis rate (%) = $100 \times$ (count of apoptotic neurons/total count of neurons). (C) The activity of caspase-3 in hippocampus was measured using a colorimetric assay kit (Abcam) according to the manufacturer's instructions. (D) Pearson's correlation analysis showed that the levels of miRNA-423-3p and miRNA-296-5p were significantly correlated with caspase-3 activity in hippocampus. All data are presented as the mean \pm SD; $n = 6$ per group.

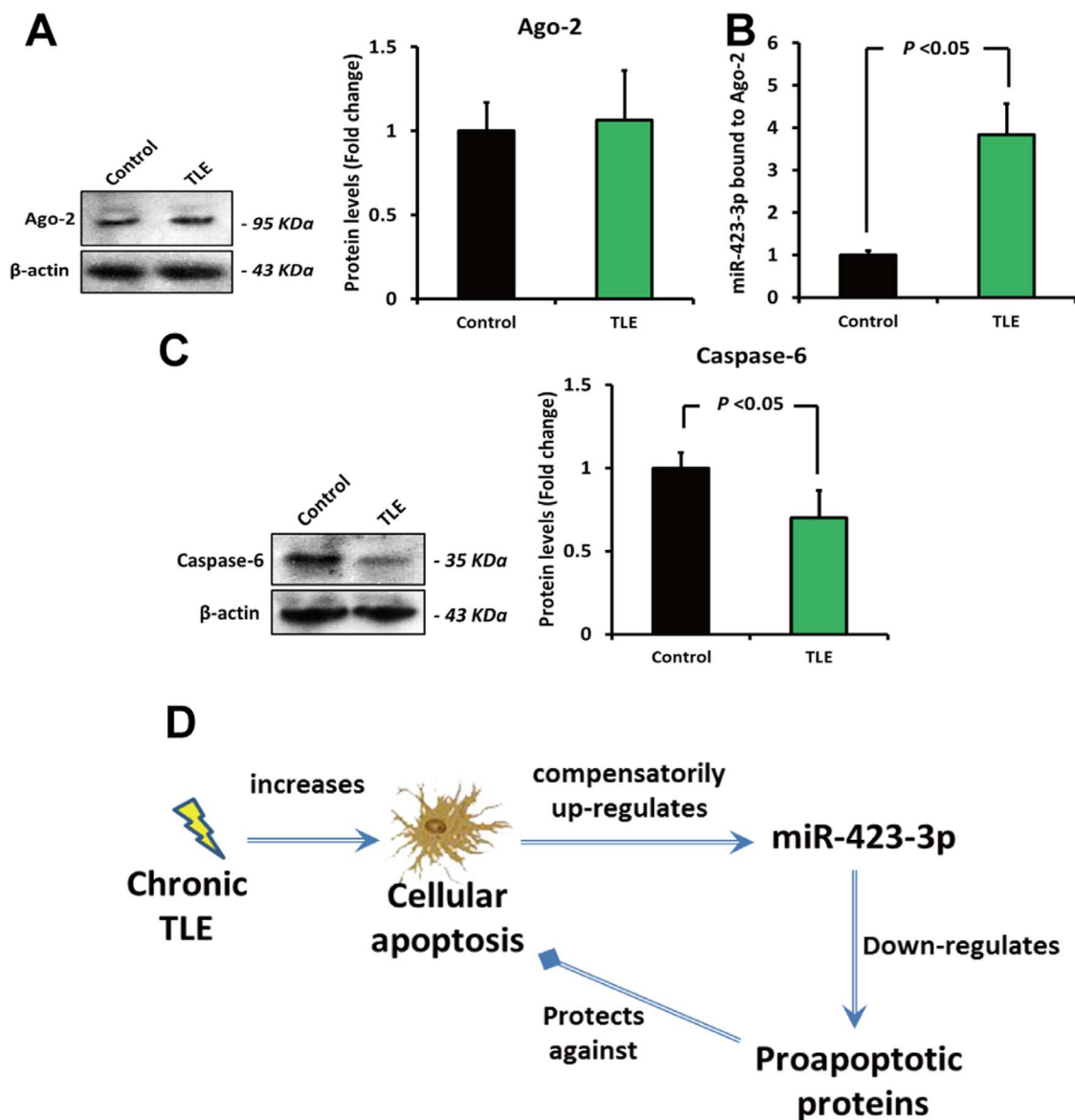


Figure 4 | Loading of miRNA-423-3p in RISC and protein levels of its predicted targets. (A) Protein levels of Ago-2, a crucial component of RISC, in hippocampus of chronic TLE rats and controls were detected by western blot (cropped gels/blots are used here, and the full-length gels and blots are shown in Supplementary Fig. S4A). (B) miRNA-423-3p levels eluted by immunoprecipitation of Ago-2 in hippocampus of chronic TLE rats and controls. (C) The protein levels of caspase-6, a predicted target of miRNA-423-3p, in hippocampus of chronic TLE rats and controls were assessed by western blot (cropped gels/blots are used here, and the full-length gels and blots are shown in Supplementary Fig. S4B). (D) Illustration showing that miR-423-3p might be compensatorily up-regulated in response to cellular apoptosis and tried to inhibit apoptosis via down-regulation of proapoptotic proteins. All data are presented as the mean \pm SD; $n = 6$ per group.

Rats were fixed in a stereotaxic apparatus (Stoelting, USA) under deep anesthesia (10% chloral hydrate, 3.5 mL/kg, i.p.). An electrodes were implanted into the right basolateral amygdala as previously described (AP: -3.0 mm; L: -4.8 mm; V: -8.8 mm)^{27,28}. The electrode was connected to a miniature receptacle, which was well embedded in the skull with screws and dental acrylic cement. After the surgery, the rats were treated with penicillin for 3 days to prevent infection and allowed to recover from surgery for 10 days.

Seizure was induced by 20 min amygdala stimulation (100 ms train of 1 ms, 60 Hz bipolar pulses, 400 μ A, every 0.5 s) using a ML1101 electronic stimulator. Electroencephalograms of the right amygdala were recorded with a digital amplifier (AD Instrument, USA). Seizure severity was assessed according to a 5-stage scale²⁹: (I) facial movement; (II) head nodding; (III) unilateral forelimb clonus; (IV) bilateral forelimb clonus and rearing; and (V) bilateral forelimb clonus and rearing and falling. Following electrical stimulation, rats were video-monitored for 2 months. The rats with chronic TLE were identified by occurrence of frequent seizures (at least 2 times IV/V spontaneous seizures per week) from 1 week after electrical stimulation^{13,15}. The time between the last spontaneous seizure and the animals were killed was 2 h. Rats in control group were handled in the same manner while did not receive any electrical stimulation.

At 2 months after amygdala stimulation, rats with chronic TLE were anesthetized with 10% chloral hydrate (3.5 mL/kg, i.p.) and were transcardially perfused with ice-cold saline. Afterwards, brains were rapidly removed and frozen in liquid nitrogen for subsequent analysis.

Total RNA was extracted by the mirVana™ miRNA Isolation Kit (Ambion, USA) according to the manufacturer's instructions. RNA quality and quantity were evaluated using Agilent 2100 Bioanalyzer. Total hippocampal RNA from rats with chronic TLE as well as control rats was pooled separately and used for miRNA sequencing ($n = 6$ for each group). The small RNAs were ligated to a 5' and a 3' adaptor sequentially and then converted to cDNA by reverse transcription. The two generated small cDNA libraries were amplified by PCR with primers complementary to the adaptor sequences. Afterwards, the libraries were deep sequenced directly using the Illumina Cluster Station and Genome Analyzer (Illumina Inc, USA) at Beijing Genomics Institute³⁰. The deep sequencing data have been deposited in NCBI SRA database and are accessible through GEO series accession number GSE52443 (<http://www.ncbi.nlm.nih.gov/geo/query/acc.cgi?acc=GSE52443>). The differences in the quantities of miRNAs were determined by comparing the \log_2 -ratio of the chronic TLE rats and control rats copies. A miRNA was considered "differentially expressed" only if it met the following criteria: (a) having at least 10 copies in either chronic TLE



or control group. (b) fold-change (\log_2) > 1.5 or fold-change (\log_2) < -1.5 between these two groups ($P < 0.05$ and $P \neq 0$). Of note, the Benjamini and Hochberg multiple testing correction was applied to adjust the P -values³¹.

To validate the initial results of high-throughput sequencing in this study, we selected miRNAs that met the following criteria for additional qRT-PCR analysis: (a) having at least 30 copies in either chronic TLE or control group. (b) Showing fold-change (\log_2) > 1.5 or fold-change (\log_2) < -1.5 between these two groups ($P < 0.01$ and $P \neq 0$). As a result, six differentially expressed miRNAs were screened out for subsequent qRT-PCR confirmation. The detailed protocol of qRT-PCR was described as previously¹⁴. All experiments were performed in triplicate.

Potential target genes of the five known miRNAs were predicted using the database of RNAhybrid and miRanda as previously described^{32–34}. Meanwhile, the potential target genes of novel miR-54 were predicted using a method described by Barozai et al.³⁵, and Wu et al.³⁶. First, we submitted the novel miRNA sequences as queries to the NCBI Basic local alignment search tool program with the following parameters: (1) database reference: RefSeq RNA; (2) organism: Rattus norvegicus; and (3) program selection: highly similar sequences (megablast). Afterwards, the mRNA sequences showing 75% query coverage were selected and submitted to RNAhybrid for the confirmation of the potential targets. Only targets having stringent seed site located at positions 2–7 from the 5' end of the miRNA along or with the supplementary site were selected and further submitted to the miRanda to reconfirm the RNAhybrid results. Additionally, the KEGG pathway database was used to filter the enriched pathways of miRNA targets.

Nissl staining was used to detect surviving neurons in hippocampus. Briefly, the frozen slices were stained with 1% cresyl violet at 50°C for 5 min as previously described³⁷, and the neurons with dark violet nucleus and intact morphology were identified as surviving neurons. Six fields of CA1 and CA3 regions in hippocampus of each section were randomly selected, and the number of surviving neurons was counted. The neuronal survival rate was defined as follows: neuronal surviving rate (%) = $100 \times (\text{count of surviving neurons} / \text{total count of neurons})$. Meanwhile, TUNEL was performed using a modified protocol described by Stähelin and colleagues to assess neuronal apoptosis³⁸. TUNEL-positive neurons with condensate nuclear were identified as apoptotic neurons^{39,40}. Six different areas were selected at random from the CA1 and CA3 regions of each section, and the number of TUNEL-positive neurons in these areas was counted. The neuronal apoptosis rate was defined as follows: neuronal apoptosis rate (%) = $100 \times (\text{count of apoptotic neurons} / \text{total count of neurons})$. In addition, the activity of caspase-3 in hippocampus was measured using a colorimetric assay kit (Abcam) according to the manufacturer's instructions.

The association between miRNAs and Ago-2, a crucial component in RISC, was investigated as described by Henshall's group^{10,41}. Briefly, the hippocampus of six rats from each group were pooled and homogenized in 0.7 ml of ice-cold immunoprecipitation buffer. The homogenate was centrifuged at $16\,000 \times g$ for 15 min at 4°C and the supernatant was retained. Antibodies against Ago-2 (1:50; Cell Signaling Technology Inc., USA) was added to 400 mg of lysate in a final volume of 1 ml, mixed and incubated overnight. Next, 20 ml of 50% Protein-A/G-agarose beads was added for 1 h at 4°C and then centrifuged at $16\,000 \times g$ for 15 min. The pellet was washed in immunoprecipitation buffer, and miRNA was extracted. Afterwards, qRT-PCR was performed to quantify the expression of miRNA.

Western blot analysis was performed as previously described^{42,43}. Briefly, hippocampus of each rat was homogenized and the total proteins were extracted by RIPA lysis buffer. Different samples with an equal amount of protein were separated on 8–12% SDS polyacrylamide gels, transferred to nitrocellulose membranes, and blocked in 5% BSA powder in $1 \times$ trisbuffered saline with 0.1% Tween 20 ($1 \times$ TBST) at room temperature for 2 h. Membranes were incubated overnight at 4°C with a mouse monoclonal antibody against Ago-2 (1:1000; Cell Signaling Technology Inc., USA) and Caspase-6 (1:800; Cell Signaling Technology Inc., USA), then washed with $1 \times$ TBST, and incubated with HRP-coupled secondary antibody for 2 h at room temperature. After washing, protein bands were detected with chemiluminescent HRP substrate (Thermo Scientific Inc., USA) for 5 min at room temperature and exposed to an X-ray film. The band intensity was analysed using Quantity One software 4.6.2 (Bio-Rad Laboratories Inc., USA) and normalized to a loading control β -actin.

Statistical analysis was conducted using the SPSS 17.0 software. Statistical differences were determined by independent sample t -test. Pearson's correlation analysis was used to investigate the correlation between the miRNA levels and caspase-3 activity. All data are expressed as mean \pm SD. $P < 0.05$ was considered statistically significant.

- Palmigiano, A., Pastor, J., Garcia de Sola, R. & Ortega, G. J. Stability of synchronization clusters and seizurability in temporal lobe epilepsy. *PLoS One* **7**, e41799 (2012).
- Geary, E. K., Seidenberg, M. & Hermann, B. Atrophy of basal ganglia nuclei and negative symptoms in temporal lobe epilepsy. *J Neuropsychiatry Clin Neurosci* **21**, 152–9 (2009).
- Meng, X. F., Yu, J. T., Song, J. H., Chi, S. & Tan, L. Role of the mTOR signaling pathway in epilepsy. *J Neurol Sci* **332**, 4–15 (2013).
- Bartel, D. P. MicroRNAs: target recognition and regulatory functions. *Cell* **136**, 215–33 (2009).
- Lagos-Quintana, M. et al. Identification of tissue-specific microRNAs from mouse. *Curr Biol* **12**, 735–9 (2002).
- Wang, W., Kwon, E. J. & Tsai, L. H. MicroRNAs in learning, memory, and neurological diseases. *Learn Mem* **19**, 359–68 (2012).
- Krichevsky, A. M., King, K. S., Donahue, C. P., Khrapko, K. & Kosik, K. S. A microRNA array reveals extensive regulation of microRNAs during brain development. *RNA* **9**, 1274–81 (2003).
- Jimenez-Mateos, E. M. & Henshall, D. C. Epilepsy and microRNA. *Neuroscience* **238**, 218–29 (2013).
- Li, M. M., Li, X. M., Zheng, X. P., Yu, J. T. & Tan, L. MicroRNAs dysregulation in epilepsy. *Brain Res* doi: 10.1016/j.brainres.2013.09.049 (2013).
- Jimenez-Mateos, E. M. et al. miRNA Expression profile after status epilepticus and hippocampal neuroprotection by targeting miR-132. *Am J Pathol* **179**, 2519–32 (2011).
- McKiernan, R. C. et al. Expression profiling the microRNA response to epileptic preconditioning identifies miR-184 as a modulator of seizure-induced neuronal death. *Exp Neurol* **237**, 346–54 (2012).
- Jimenez-Mateos, E. M. et al. Hippocampal transcriptome after status epilepticus in mice rendered seizure damage-tolerant by epileptic preconditioning features suppressed calcium and neuronal excitability pathways. *Neurobiol Dis* **32**, 442–53 (2008).
- Hu, K. et al. MicroRNA expression profile of the hippocampus in a rat model of temporal lobe epilepsy and miR-34a-targeted neuroprotection against hippocampal neuron cell apoptosis post-status epilepticus. *BMC Neurosci* **13**, 115 (2012).
- Sun, Z. et al. Genome-Wide microRNA Profiling of Rat Hippocampus after Status Epilepticus Induced by Amygdala Stimulation Identifies Modulators of Neuronal Apoptosis. *PLoS One* **8**, e78375 (2013).
- Gorter, J. A. et al. Hippocampal subregion-specific microRNA expression during epileptogenesis in experimental temporal lobe epilepsy. *Neurobiol Dis* **62**, 508–20 (2014).
- Bot, A. M., Debski, K. J. & Lukasiuk, K. Alterations in miRNA Levels in the Dentate Gyrus in Epileptic Rats. *PLoS One* **8**, e76051 (2013).
- Nissinen, J., Halonen, T., Koivisto, E. & Pitkanen, A. A new model of chronic temporal lobe epilepsy induced by electrical stimulation of the amygdala in rat. *Epilepsy Res* **38**, 177–205 (2000).
- Friedlander, M. R. et al. Discovering microRNAs from deep sequencing data using miRDeep. *Nat Biotechnol* **26**, 407–15 (2008).
- Inukai, S., de Lencastre, A., Turner, M. & Slack, F. Novel microRNAs differentially expressed during aging in the mouse brain. *PLoS One* **7**, e40028 (2012).
- Risbud, R. M. & Porter, B. E. Changes in microRNA expression in the whole hippocampus and hippocampal synaptoneurosome fraction following pilocarpine induced status epilepticus. *PLoS One* **8**, e53464 (2013).
- Houseweart, M. K. et al. Apoptosis caused by cathepsins does not require Bid signaling in an in vivo model of progressive myoclonus epilepsy (EPM1). *Cell Death Differ* **10**, 1329–35 (2003).
- Wang, Y. et al. alpha-Amino-3-hydroxy-5-methylisoxazole-4-propionic acid subtype glutamate receptor (AMPA) endocytosis is essential for N-methyl-D-aspartate-induced neuronal apoptosis. *J Biol Chem* **279**, 41267–70 (2004).
- Henshall, D. C. & Simon, R. P. Epilepsy and apoptosis pathways. *J Cereb Blood Flow Metab* **25**, 1557–72 (2005).
- Lewis, D. V. Losing neurons: selective vulnerability and mesial temporal sclerosis. *Epilepsia* **46 Suppl** **7**, 39–44 (2005).
- Daniel, N. N. & Korsmeyer, S. J. Cell death: critical control points. *Cell* **116**, 205–19 (2004).
- Henshall, D. C. Apoptosis signalling pathways in seizure-induced neuronal death and epilepsy. *Biochem Soc Trans* **35**, 421–3 (2007).
- Zhang, Q. et al. Anticonvulsant effect of unilateral anterior thalamic high frequency electrical stimulation on amygdala-kindled seizures in rat. *Brain Res Bull* **87**, 221–6 (2012).
- Sun, Z. et al. Activation of Adenosine Receptor Potentiates the Anticonvulsant Effect of Phenytoin against Amygdala Kindled Seizures. *CNS Neurol Disord Drug Targets* doi:10.2174/18715273113129990078 (2013).
- Racine, R. J. Modification of seizure activity by electrical stimulation: II. Motor seizure. *Electroencephalogr Clin Neurophysiol* **32**, 281–94 (1972).
- Yu, J. T. et al. Triggering receptor expressed on myeloid cells 2 variant is rare in late-onset Alzheimer's disease in Han Chinese individuals. *Neurobiol Aging* **35**, 937.e1–3 (2014).
- Benjamini, Y., Drai, D., Elmer, G., Kafkafi, N. & Golani, I. Controlling the false discovery rate in behavior genetics research. *Behav Brain Res* **125**, 279–84 (2001).
- Rehmsmeier, M., Steffen, P., Hochsmann, M. & Giegerich, R. Fast and effective prediction of microRNA/target duplexes. *RNA* **10**, 1507–17 (2004).
- Enright, A. J. et al. MicroRNA targets in Drosophila. *Genome Biol* **5**, R1 (2003).
- Min, H. & Yoon, S. Got target? Computational methods for microRNA target prediction and their extension. *Exp Mol Med* **42**, 233–44 (2010).
- Barozai, M. Y. Identification and characterization of the microRNAs and their targets in Salmo salar. *Gene* **499**, 163–8 (2012).
- Wu, Q., Wang, C., Guo, L., Ge, Q. & Lu, Z. Identification and characterization of novel microRNA candidates from deep sequencing. *Clin Chim Acta* **415**, 239–44 (2013).
- Jiang, T. et al. Triggering receptor expressed on myeloid cells 2 knockdown exacerbates aging-related neuroinflammation and cognitive deficiency in senescence-accelerated mouse prone 8 mice. *Neurobiol Aging* **35**, 1243–51 (2014).



38. Stahelin, B. J., Marti, U., Solioz, M., Zimmermann, H. & Reichen, J. False positive staining in the TUNEL assay to detect apoptosis in liver and intestine is caused by endogenous nucleases and inhibited by diethyl pyrocarbonate. *Mol Pathol* **51**, 204–8 (1998).
39. Jiang, T. *et al.* Angiotensin-(1–7) modulates renin-angiotensin system associated with reducing oxidative stress and attenuating neuronal apoptosis in the brain of hypertensive rats. *Pharmacol Res* **67**, 84–93 (2013).
40. Jiang, T. *et al.* Temsirolimus promotes autophagic clearance of amyloid- β and provides protective effects in cellular and animal models of Alzheimer's disease. *Pharmacol Res* **81**, 54–63 (2014).
41. Sano, T. *et al.* MicroRNA-34a upregulation during seizure-induced neuronal death. *Cell Death Dis* **3**, e287 (2012).
42. Jiang, T. *et al.* Suppressing inflammation by inhibiting the NF-kappaB pathway contributes to the neuroprotective effect of angiotensin-(1-7) in rats with permanent cerebral ischaemia. *Br J Pharmacol* **167**, 1520–32 (2012).
43. Jiang, T. *et al.* Acute metformin preconditioning confers neuroprotection against focal cerebral ischemia by pre-activation of AMPK-dependent autophagy. *Br J Pharmacol* doi: 10.1111/bph.12655 (2014).

Acknowledgments

This work was supported by the grants from the National Natural Science Foundation of China to Lan Tan (81171209, 81371406) and Jin-Tai Yu. (81000544), the grants from the Shandong Provincial Natural Science Foundation to Lan Tan (ZR2011HZ001) and Jin-Tai Yu. (ZR2010HQ004), the Medicine and Health Science Technology Development Project of Shandong Province to Lan Tan (2011WSA02018) and Jin-Tai Yu. (2011WSA02020), and

the Innovation Project for Postgraduates of Jiangsu Province to Teng Jiang (CXLX13_561). The authors would like to thank Lin Tan, Qiu-Yan Liu, Zhong-Chen Wu and Xiao-Ling Zhong for technical assistance.

Author contributions

J.T.Y. and L.T. design the whole study. M.M.L. and Z.S. performed the experiment. Q.Z. and C.C.T. analyzed the data. T.J. wrote the main manuscript text and prepared all figures. All authors reviewed the manuscript.

Additional information

Supplementary information accompanies this paper at <http://www.nature.com/scientificreports>

Competing financial interests: The authors declare no competing financial interests.

How to cite this article: Li, M.-M. *et al.* Genome-wide microRNA expression profiles in hippocampus of rats with chronic temporal lobe epilepsy. *Sci. Rep.* **4**, 4734; DOI:10.1038/srep04734 (2014).



This work is licensed under a Creative Commons Attribution-NonCommercial-ShareAlike 3.0 Unported License. The images in this article are included in the article's Creative Commons license, unless indicated otherwise in the image credit; if the image is not included under the Creative Commons license, users will need to obtain permission from the license holder in order to reproduce the image. To view a copy of this license, visit <http://creativecommons.org/licenses/by-nc-sa/3.0/>